

# Revealing the true incidence of pandemic A(H1N1)pdm09 influenza in Finland during the first two seasons

Mikhail Shubin, Artem Lebedev, Outi Lyytikäinen, Kari Auranen

## Supplement 4: Additional results

The pictures in this Supplement illustrate additional results: posterior distribution of the parameters  $d^{(\text{hosp})}$ ,  $d_t^{(\text{mild})}$ ,  $w_t$ ; realised reproduction number  $R_t$ ; detection ratio per week; posterior distribution of the number of infections by age group; correlation between the parameters. All distributions are visualized with more probable values represented by more concentrated color. In addition, a few samples from the distributions are shown.

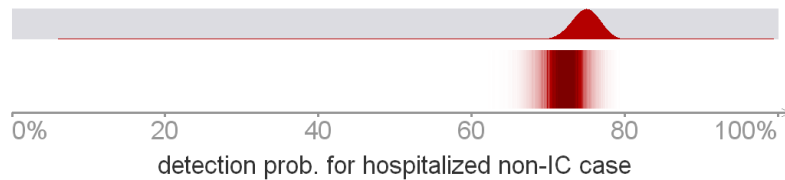


Figure 1: **The posterior distribution of the detection probability for the hospitalized cases  $d^{(\text{hosp})}$ .** The prior distribution for the  $d^{(\text{hosp})}$  is shown for reference.

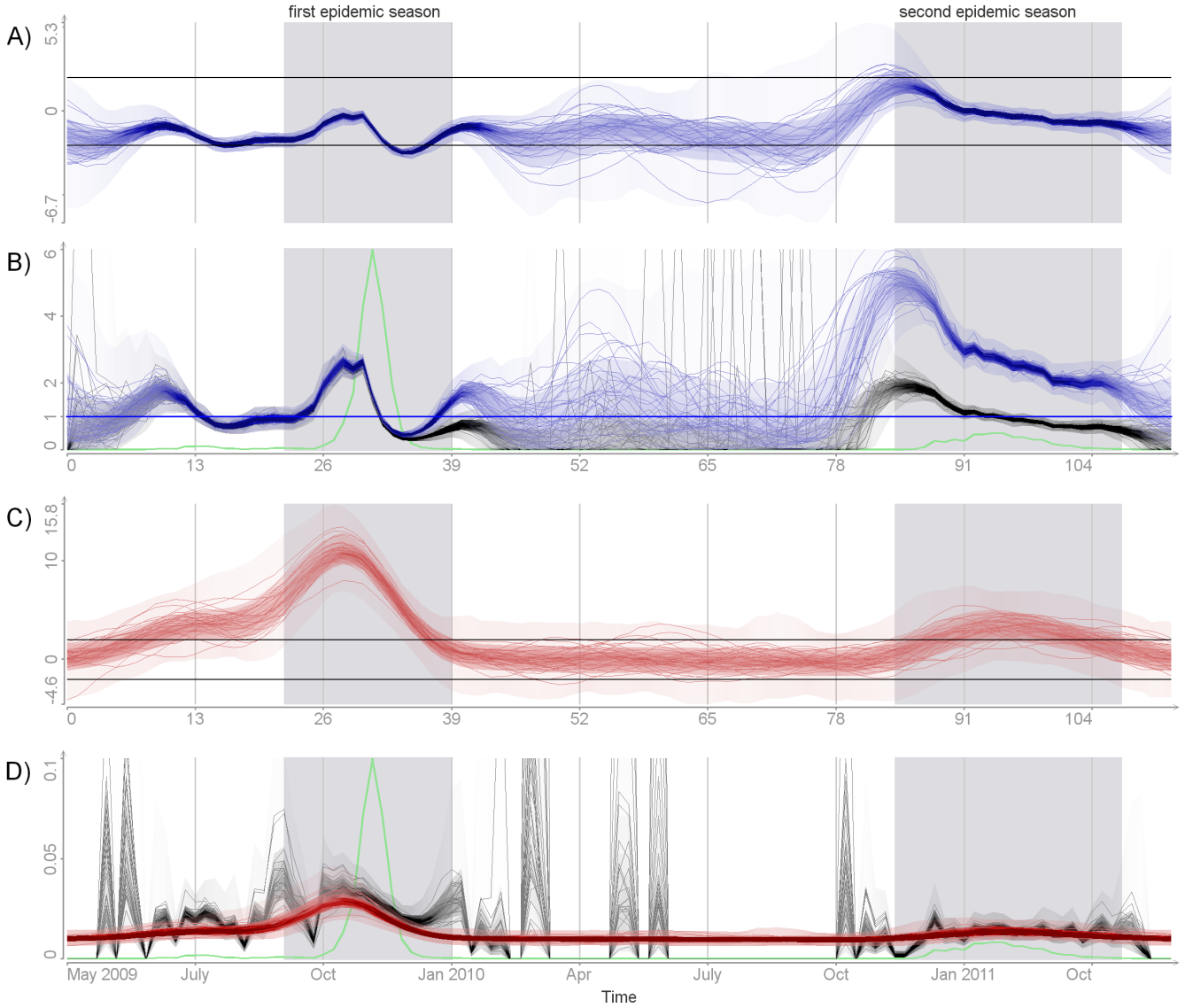


Figure 2: **The posterior distribution of the time-dependent variables.** Panel A: parameter  $\varepsilon_t$  (transformed  $w_t$ ). The black horizontal lines mark 95% prior credible interval. Panel B: Basic reproduction number  $R_{0,t}$  (blue lines, duplicated from the main text) and the realized reproduction number  $R_t$  (black lines). The realized  $R_t$  was estimated as  $I_t / (I_{t-1} - \sum q_a S_a)$  for  $(I_{t-1} - \sum q_a S_a) > 0$ . The denominator represent the number of new infections introduced through within-population transmission. The green lines show the numbers of observed cases (not to scale). Panel C: parameter  $\delta_t$  (transformed  $d_t^{(\text{mild})}$ ). The black horizontal lines mark 95% prior credible interval. Panel D: detection probability for the mild cases  $d_t^{(\text{mild})}$  (red lines, duplicated from the main text) and the detection ratio  $D_t/I_t$  (black lines). Green line shows the numbers of observed cases (not to scale).

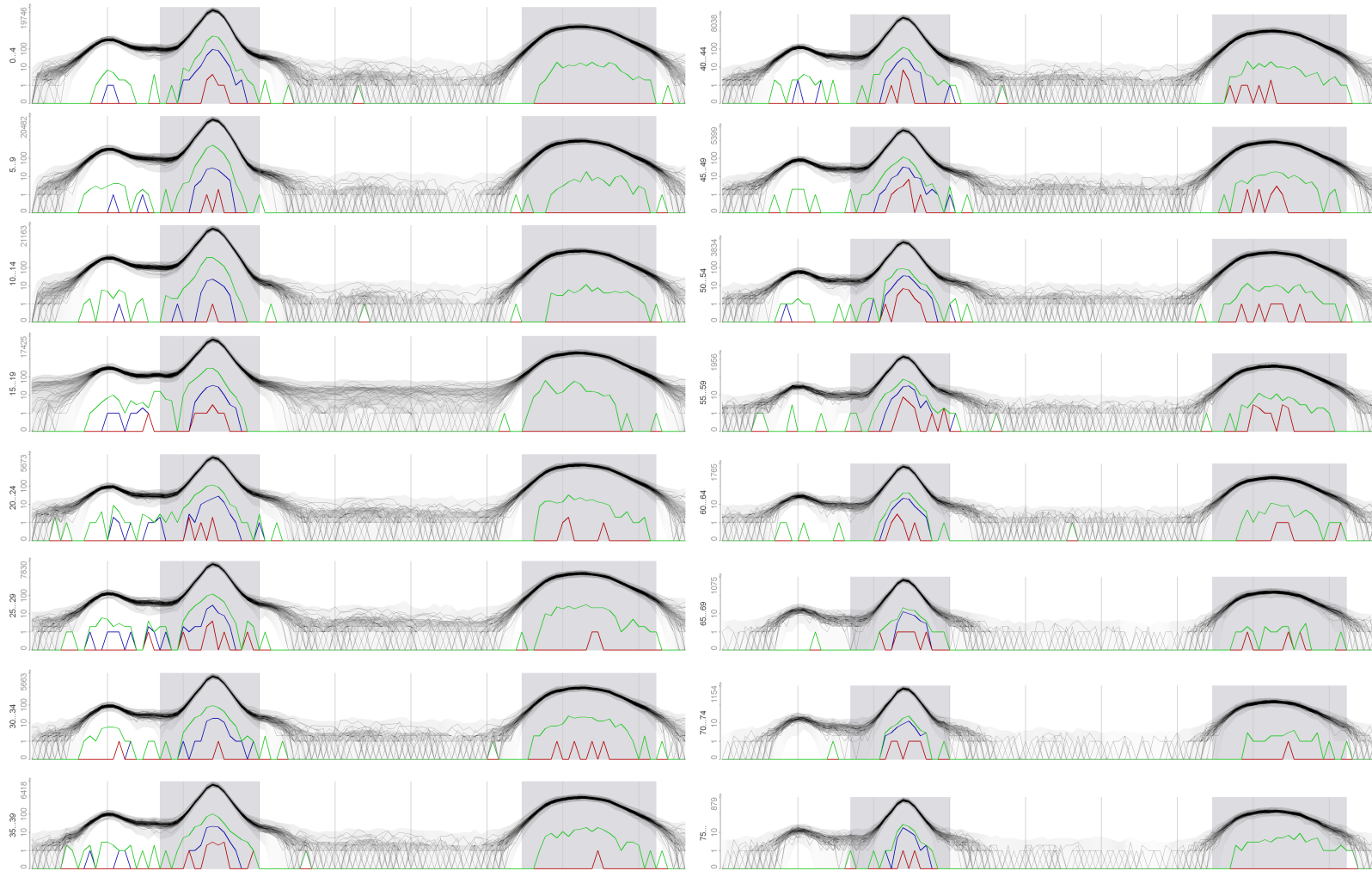


Figure 3: **Posterior distribution of the number of infections per week.** Each subplot presents a single age group. Solid lines represent the total numbers of observed cases (green), numbers of observed hospitalized cases (blue) and IC cases (red);

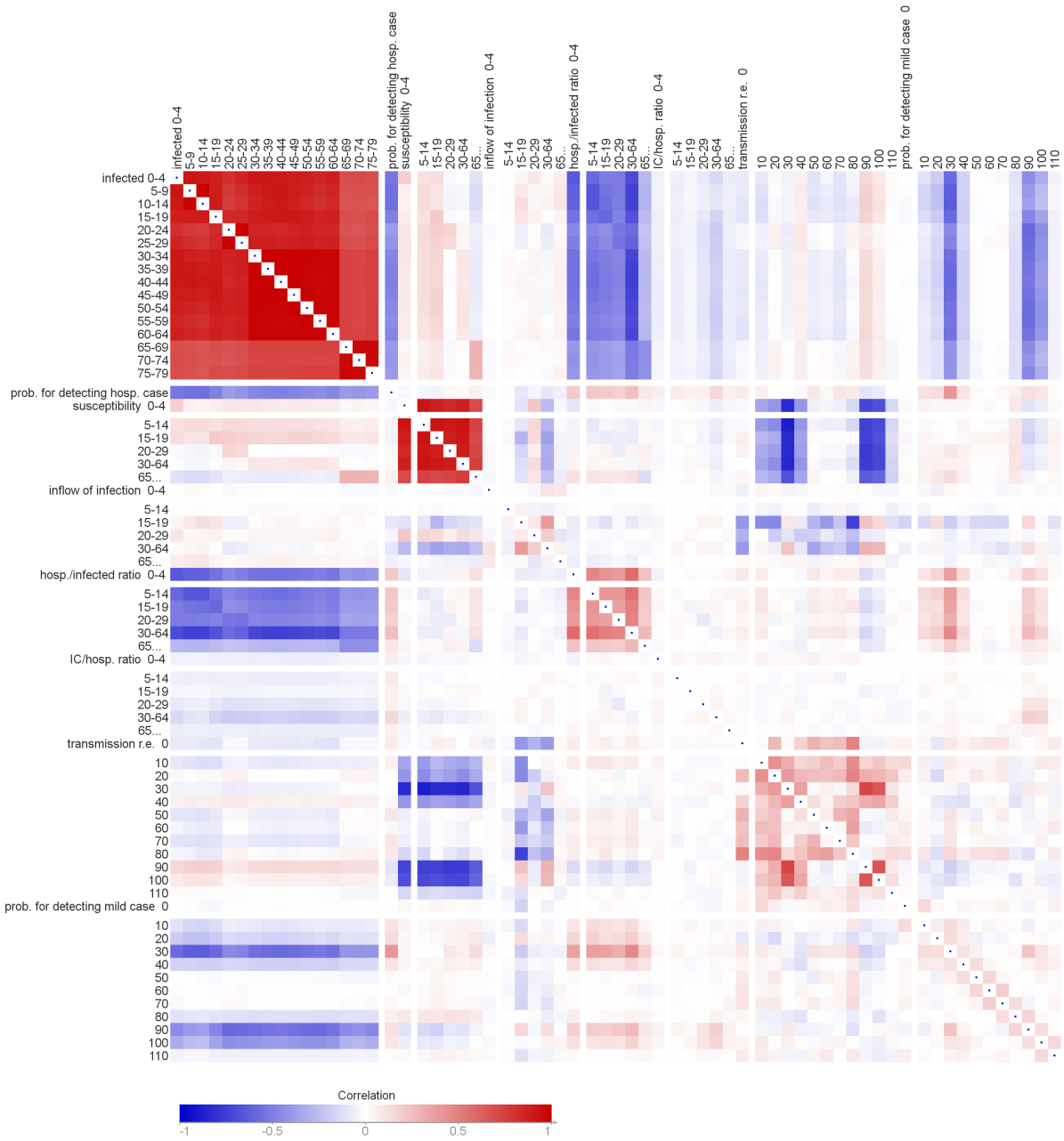


Figure 4: **Pearson Correlation matrix for some of the models unknowns.** The estimated numbers of infections and the susceptibility parameters  $p_a$  in different age groups have strong posterior correlation. There is negative posterior correlation between  $p_a$  and the transmission random effect  $w_t$  (see Fig. 5 for details). There is no strong correlation between the random effects  $w_t$  and  $d_t^{(\text{mild})}$ .

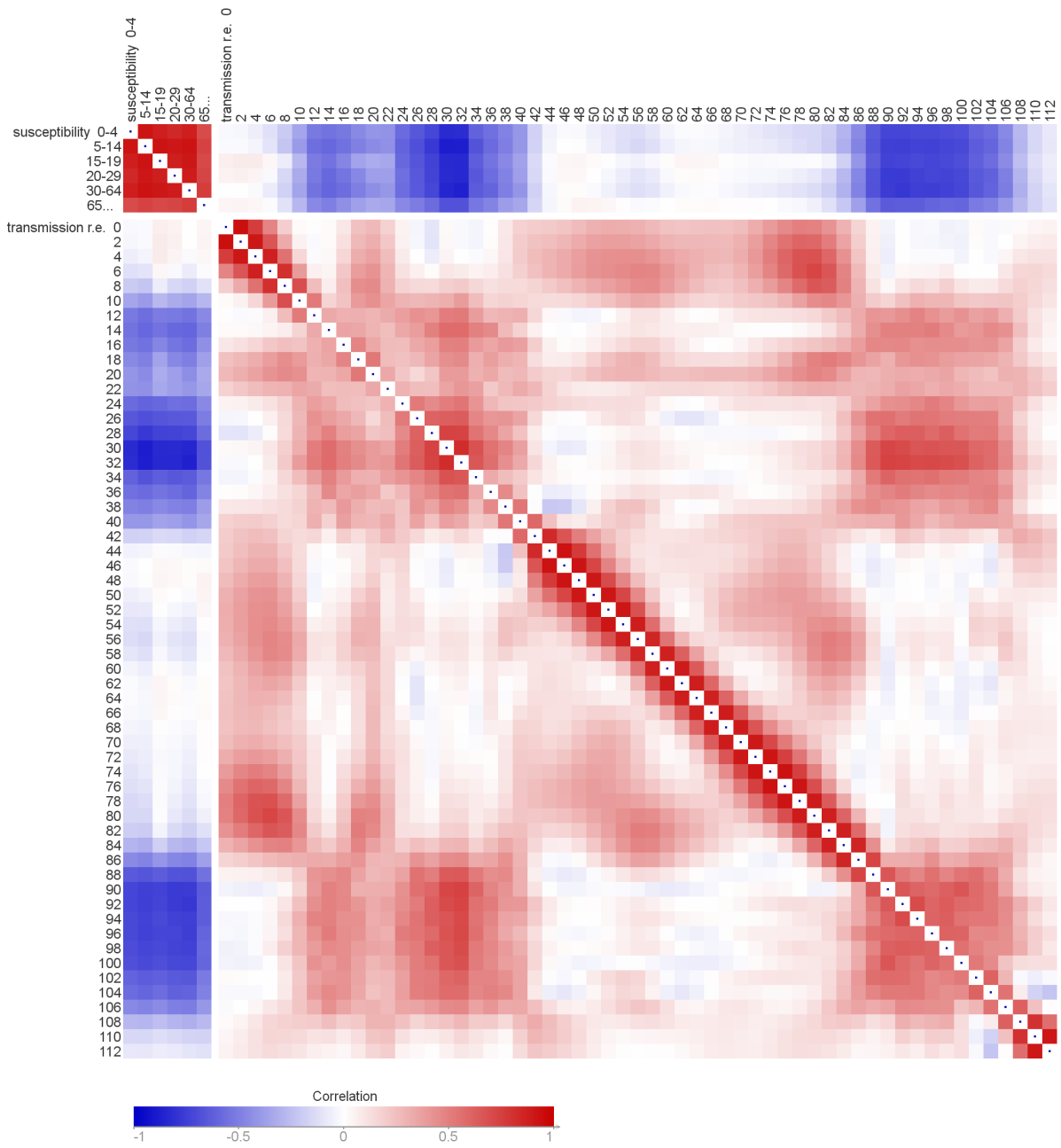


Figure 5: **Pearson Correlation matrix for the susceptibility parameters  $p_a$  and the transmission random effect  $w_t$ .** Parameters  $p_a$  show strong negative correlation with  $w_t$  around the peak of the first season ( $t \simeq$  week 30) and the second season ( $t \simeq$  week 90). The values of  $w_t$  are positively correlated.

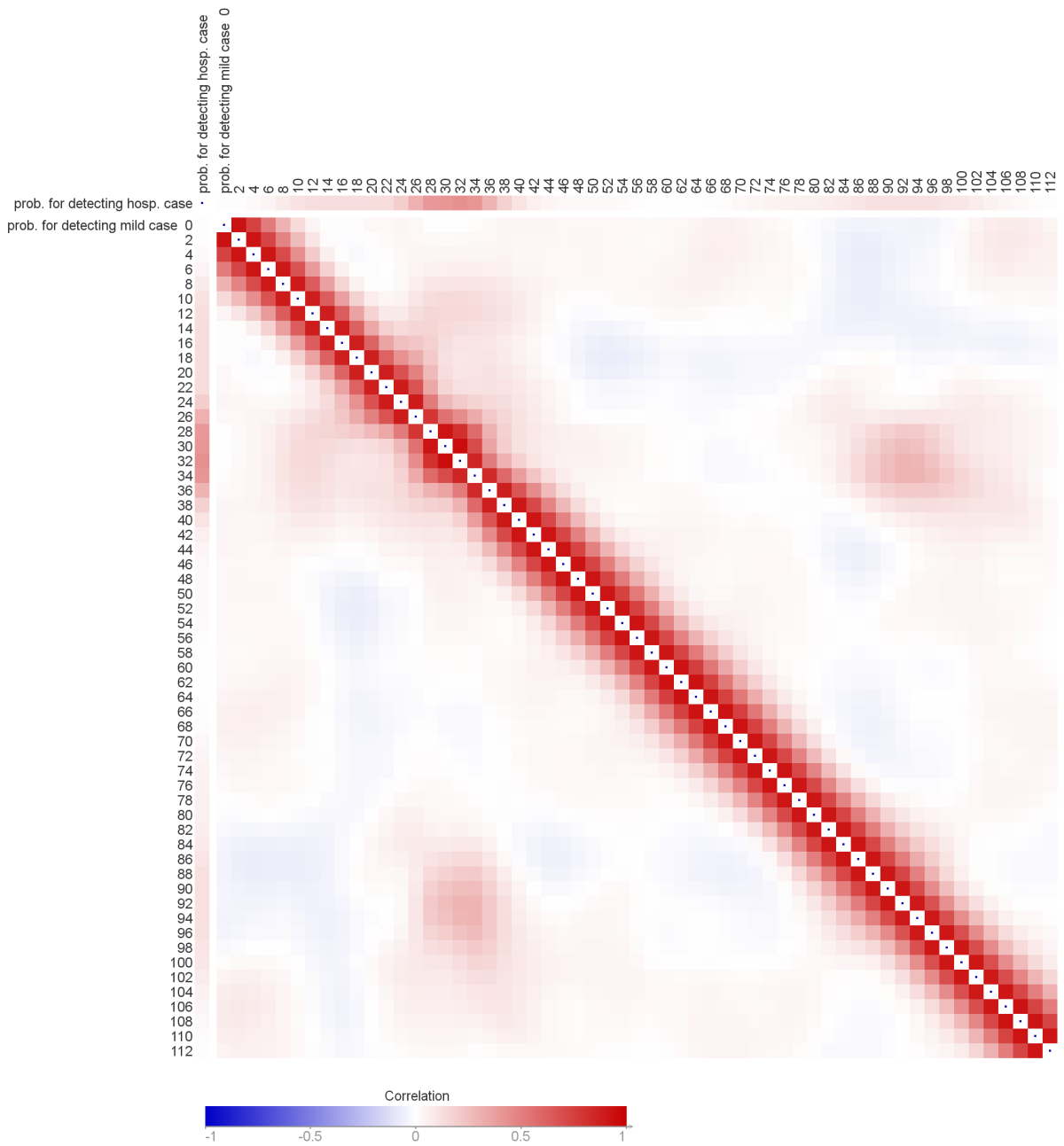


Figure 6: **Pearson Correlation matrix for the detection probabilities  $d_t^{(\text{mild})}$  and  $d_t^{(\text{hosp})}$ .** The values of  $d_t^{(\text{mild})}$  for the adjacent weeks are strongly correlated, reflecting the smoothness of the process.